Journal of Zhejiang University-SCIENCE A (Applied Physics & Engineering)
ISSN 1673-565X (Print); ISSN 1862-1775 (Online)
www.jzus.zju.edu.cn; www.springerlink.com
E-mail: jzus@zju.edu.cn

Experimental study on the mechanical behavior and deformation characteristics of gravel cushion in an immersed tube tunnel*

Wei-le CHEN†[1], Chao GUO[2], Xiao HE[2], Bai-yong FU[2], Jian LIU[1]

[1]*Shenzhen-Zhongshan Link Administration Center, Zhongshan 528400, China*

[2]*CCCC Highway Bridges National Engineering Research Center Co., Ltd., Beijing 100088, China*

†E-mail: 809487716@qq.com

Received Sept. 16, 2019; Revision accepted Dec. 24, 2019; Crosschecked June 15, 2020

Abstract: The immersed tube tunnel section of the Shenzhen-Zhongshan Link exhibits complex geological conditions and high back sludge strength. The tunnel cushion adopts the gravel and flaky stone combined cushion. The major influencing factors of the mechanical deformation characteristics of the gravel and flaky stone composite cushion are studied through a physical model experiment. The following results are reported. (1) The load–settlement curves of the flaky stone cushion become more compact with a dense increment under the design load. These curves can be regarded as nonlinear mechanical characteristics. The load–settlement curves of the gravel cushion and the gravel and flaky stone composite cushion exhibit the characteristics of a two-stage linear change. (2) The flatness of the top of flaky stone cushion considerably affects settlement and secant modulus. The flatness of the top of flaky stone should be ensured during construction. (3) Gradation and thickness exert no evident effect on the compressibility of a cushion. The preloading pressure caused by the construction height difference of the cushion materials plays an important role in improving the initial stiffness of a cushion and reducing initial settlement and overall settlement. (4) This study investigates the preloading under 30 kPa of the 0.7-m flaky stone and 1.0-m gravel combination cushion. It recommends the following secant modulus values: 48.89 MPa for the section of 0–30 kPa and 10.47 MPa for the section of 30–110 kPa.

Key words: Immersed tube tunnel; Gravel cushion; Model experiment; Deformation characteristics
https://doi.org/10.1631/jzus.A1900408 **CLC number:** TU472.21

1 Introduction

An immersed tube tunnel is an important type of channel across rivers and seas. The stress and deformation mechanism of such a tunnel has been clarified (Ranjith and Narasimhan, 1996; Zhang et al., 2011). After years of engineering practice (Glerum, 1995; Gursoy, 1995; Rasmussen and Grantz, 1997), this structure is insensitive to settlement but extremely sensitive to the differential settlement of the foundation (Zhong et al., 2007; Li and Chen, 2011; Xu et al., 2015; Su et al., 2018). The construction of an underwater foundation trench is difficult and concealed. Therefore, the precision of trenching makes achieving the design requirements challenging, and a layer of cushion must be laid between the bottom of the tunnel and the bottom of the trench to ensure the flatness of the tunnel foundation (Xu et al., 1995; Fu, 2004; Zhou et al., 2012; Yang, 2015). The differential settlement of an immersed tube tunnel is composed of the uneven settlement of each pipe section, and the settlement of an immersed tube tunnel includes the settlement of the foundation soil and the cushion.

The Shenzhen-Zhongshan Link immersed tube tunnel passes through various layers. Its geological conditions are complex, and siltation strength at the site is high. Excessive silting increases the back silting content in the submerged tube cushion,

* Project supported by the National Key Research and Development Program of China (Nos. 2018YFC0809600 and 2018YFC0809602)
ORCID: Wei-le CHEN, https://orcid.org/0000-0002-4839-6652

reducing the bearing capacity of the cushion (Grantz, 2001; Li et al., 2002; Xie et al., 2014; Xue, 2018; He and Xin, 2019). Therefore, the selection of the tunnel cushion layer should not only consider the flatness of the foundation but should also ensure the capacity of the cushion to hold silt, which is suitable for dredging the cushion layer.

The design of the gravel cushion in the Shenzhen-Zhongshan Link immersed tube tunnel includes a two-layer structure. The upper layer is a 1-m thick gravel cushion, and the lower layer is a 0.7-m thick flaky stone layer (Fig. 1). The primary purpose of leveling off the flaky stone is to reduce the influence of groove silting, which is beneficial for clearing surface back silt. The bottom width of the leveled-off flaky stone layer is flush with the width of the bottom of the groove. The width is the same as the bottom slope of the groove.

The flaky stone is a type of stone between heavy rocks and gravel. The size of a flaky stone considerably differs from that of gravel. Many domestic and overseas projects use gravel as cushion material (Chen and Zhou, 2013; Zhang XJ et al., 2013; Zhang ZG et al., 2018). Numerous studies have been conducted on the mechanical deformation characteristics of gravel cushion. The construction technology and mechanical deformation characteristics of gravel cushion are relatively clear (Yang et al., 2014; Yue, 2014; Wang, 2015; Feng and Yin, 2018). However, at present, no example has used a combination of flaky stone and gravel cushion in an immersed tube tunnel because the mechanical deformation characteristics of a flaky stone and gravel combination cushion remain unclear.

A mechanical performance test of the flaky stone and gravel cushion combination scheme is conducted in this study through indoor physical and mechanical model tests based on the Shenzhen-Zhongshan Link. The influences of laying thickness, gradation, and preloading pressure caused by the chute method are quantitatively analyzed. This study proposes a structural scheme for gravel cushion, the corresponding secant modulus, the bearing capacity, and other mechanical indexes, providing scientific basis for reasonably determining cushion thickness and feasible construction technology, accurately evaluating foundation stiffness deviation, and ensuring the stress safety of an immersed tube structure.

2 Experiment

2.1 Experimental device

The experimental device includes four parts: the experiment box with a furrow mold, the load plate, the experimental material, and the experimental equipment and auxiliary equipment.

This experiment adopts a limited vertical loading method. The width of the furrow design is 1.2 m, the width of the ridge design is 1.8 m, and the maximum

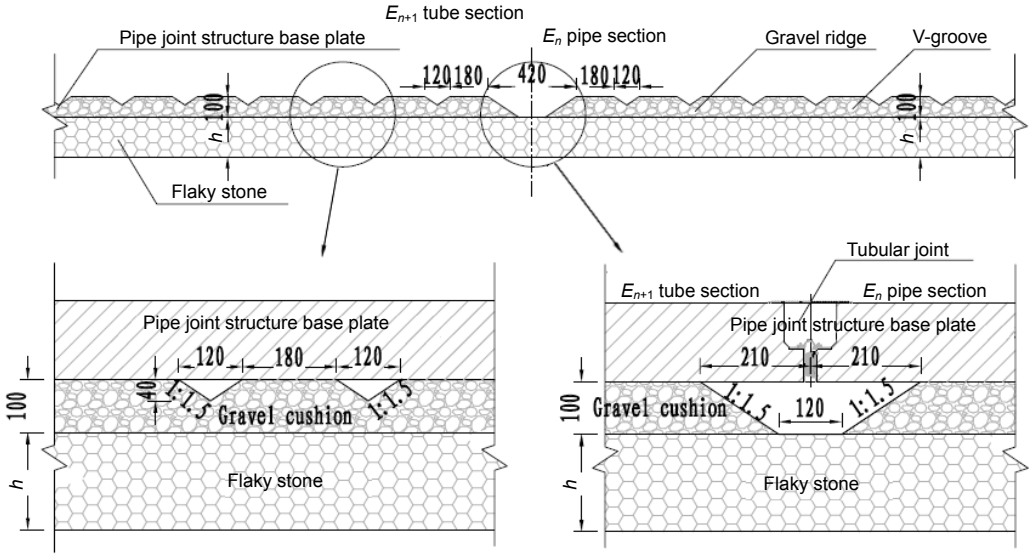

Fig. 1 Vertical sectional view of the gravel cushion layout (unit: cm)

E_n and E_{n+1} indicate the former and latter immersed tube tunnels, respectively; h is the thickness of flaky stone

filling thickness of the cushion is 1.7 m. The dimension of the model box is 3.0 m (length)×3.0 m (width)×1.8 m (height). The furrow mold is designed in accordance with the furrow structure. The mold material is made of a steel plate with a thickness of 2 cm. The mold is welded with ribs, and the center distance between the ribs is 0.58 m. Refer to Fig. 2 for details.

The plane size of the upper loading plate (Fig. 3) of the gravel cushion is determined to be 2.2 m×3.0 m in accordance with the single-ridge width of the stone ridge. To reasonably simulate the structure of an immersed tube tunnel, the loading plate is made of reinforced concrete material with a thickness of not less than 0.2 m, and a strength greater than that of C50. The diameter of the steel bar is 20 mm, the spacing between the steel bars is 200 mm, and the spacing between the upper and lower layers of the steel mesh is 160 mm.

Fig. 2 Experimental device box

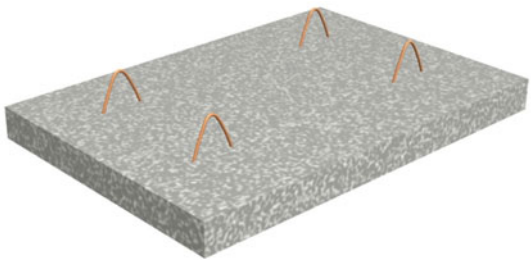

Fig. 3 Loading plate

The same gravel and flaky stone are used during the experiment.

The experimental equipment and auxiliary equipment include the loading system, displacement meter, forklifts, sieve set, laser level, and steel tape. The loading device is shown in Fig. 4. The maximum vertical load force reaches 200 t.

Fig. 4 Loading device

2.2 Experimental method

2.2.1 Conditions

First, physical model tests are conducted on flaky stone and gravel to determine their mechanical deformation characteristics. Combined with the test results, targeted tests of composite flaky stone and gravel cushion are then performed to analyze the influences of laying thickness, grading, preloading pressure, and other factors of flaky stone and gravel cushion.

The experimental scheme for the flaky stone layer is shown in Table 1. B1-1, B1-2, and B1-3 are the standard conditions. A 1-m thick gravel cushion is set above the flaky stone layer. By conducting B1-4 and B1-5 experiments, the influence of the contact state of the flaky stone and the loading plate is analyzed. The drop pressure during the underwater laying of a 1-m thick gravel cushion is 40 kPa. The effects of the preloading pressure are analyzed by conducting two sets of experiments, namely, B1-6 and B1-7. Particle grading is another important parameter of the experimental material. The effects of particle grading are analyzed by conducting experiments on two sets of conditions, namely, B1-8 and B1-9.

In the gravel cushion experiment (Table 2), the height of the chute is 3 m, and the thickness of the cushion layer is 1.0 m or 1.7 m. The other experimental conditions remain the same. The effects of the gravel cushion thickness on the physical properties of

Table 1 Experimental method for flaky stone

Working condition	Grading (mm)	Cushion thickness (m)	Preloading pressure (kPa)	Stone ridge size
B1-1	80–200	0.7+0	0	3 m without ditch
B1-2	80–200	0.7+0	0	3 m without ditch
B1-3	80–200	0.7+0	0	3 m without ditch
B1-4	80–200	0.7+0	0	3 m without ditch, top gravel leveled off
B1-5	80–200	0.7+0	0	3 m without ditch, top gravel leveled off
B1-6	80–200	0.7+0	40	3 m without ditch, top gravel leveled off
B1-7	80–200	0.7+0	40	3 m without ditch, top gravel leveled off
B1-8	80–200	0.7+0	40	3 m without ditch
B1-9	50–100	0.7+0	30	3 m without ditch

Table 2 Experimental method for gravel

Working condition	Grading (mm)	Cushion thickness (m)	Preloading pressure (kPa)	Stone ridge size (m)
B2-1	20–40	1.0	30	1.8×1.2
B2-2	20–40	1.0	30	1.8×1.2
B2-3	20–40	1.0	30	1.8×1.2
B2-4	20–40	1.7	30	1.8×1.2

the gravel cushion are obtained by analyzing the experimental results under different conditions.

The combination cushion adopts 0.7-m flaky stone and 1.0-m gravel. The chute height is 3 m, the preloading pressure is 30 kPa, and the other conditions remain the same (Table 3).

2.2.2 Loading process

The step loading method is adopted (Table 4). The load on the load plate top is divided into at least eight uniform vertical loading levels. After each level, the relative vertical displacement is measured from four monitoring points.

When one of the following conditions occurs, loading should be aborted. (1) The cushioning stone around the loading plate is evidently laterally extruded. (2) The load–settlement curve is maintained at a certain level. (3) The sedimentation amount is rapidly increased. (4) Loading is under a certain level. The sedimentation rate cannot reach a stable level within 24 h. When one of the aforementioned conditions is satisfied, the corresponding previous loading level can be determined as the ultimate bearing capacity.

The unloading process is divided into four uniform unloading levels, and the unloading continues until the load value at the top of the loading plate is 0 kPa.

Table 3 Flaky stone and gravel combination cushion experiment under different working conditions

Working condition	Grading (mm)	Cushion thickness (m)	Preloading pressure (kPa)	Stone ridge size (m)
B3-1	Flaky stone: 80–200; gravel: 20–40	0.7+1.0	30	Flaky stone: fully filled; gravel: 1.8×1.2
B3-2	Flaky stone: 80–200; gravel: 20–40	0.7+1.0	30	Flaky stone: fully filled; gravel: 1.8×1.2
B3-3	Flaky stone: 50–100; gravel: 20–40	0.7+1.0	30	Flaky stone: fully filled; gravel: 1.8×1.2

Table 4 Load step of the loading process

Load sequence	Loading set (kPa)
First-level loading	15
Second-level loading	30/40
Third-level loading	60
Fourth-level loading	90
Fifth-level loading	120
Sixth-level loading	150
Seventh-level loading	180
Eighth-level loading	210
Ninth-level loading	240
Tenth-level loading	270

2.3 Experimental procedure

The experimental procedures are illustrated in Fig. 5.

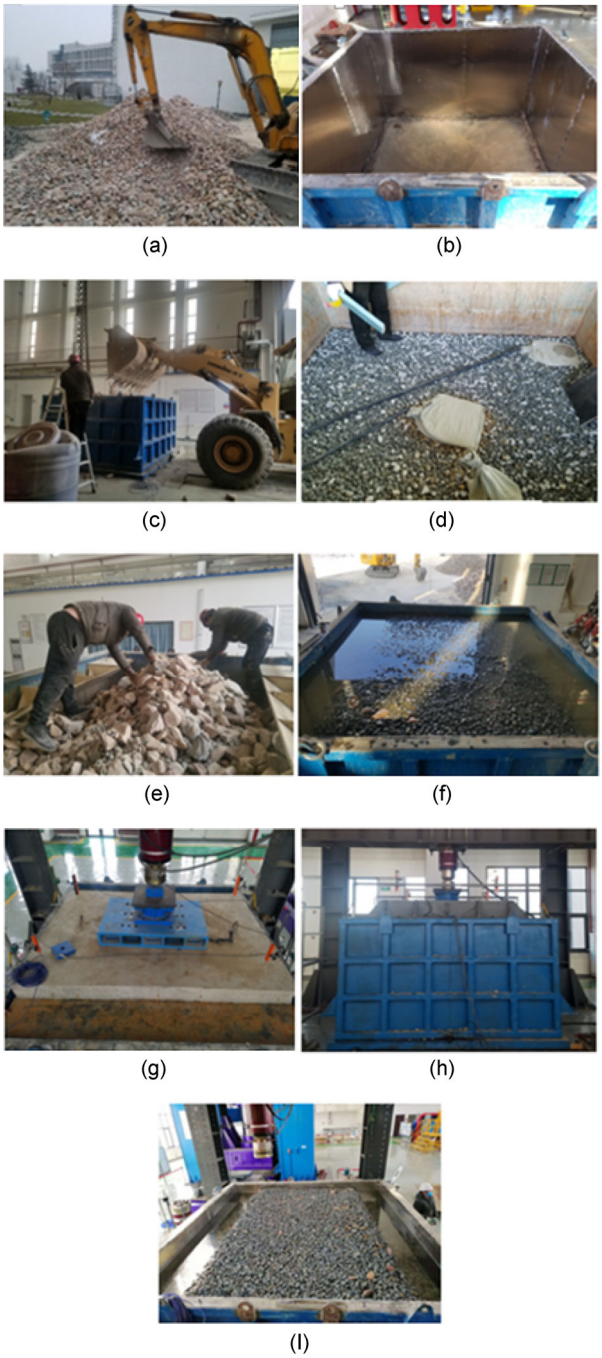

Fig. 5 Experimental procedure

(a) Gravel agitation; (b) Model box in place; (c) Model box loading; (d) Earth pressure box; (e) Leveling of gravel top; (f) Cushion water injection; (g) Loading plate and displacement sensor installation; (h) Load; (I) Gravel state after loading

3 Secant modulus calculation method

Controlling differential settlement is a key issue in the design and construction of an immersed tube tunnel. The settlement calculation method commonly used in engineering is the stratified summation method. The principle is based on the vertical stress of soil combined with the compression curve, compression index, and compression mode. The stratified settlement amount is calculated, and the sum of the settlements is used to obtain the total settlement of the foundation.

The secant modulus, which is an important parameter for calculating foundation settlement, is typically obtained through laboratory experiments. Under the condition of confined pressure, the secant modulus is the ratio of the vertical additional stress to the corresponding strain increment. Therefore, the secant modulus of the cushion obtained in this study is the secant modulus under the lateral restriction condition.

$$E_S=\frac{\sigma_S}{\varepsilon_S}=\frac{P_2-P_1}{\frac{H_2-H_1}{H_1}}=\frac{P_2-P_1}{\frac{e_1-e_2}{1+e_1}}=\frac{1+e_1}{a}, \tag{1}$$

where E_S is the secant modulus of soil, σ_S is the vertical additional stress of soil, ε_S is the strain increment that corresponds to additional stress, P_1 is the initial pressure, P_2 is the end pressure, H_1 is the height of the soil sample when soil is subjected to pressure P_1, H_2 is the height of the soil sample when soil is subjected to pressure P_2, e_1 is the void ratio of soil after compression and stabilization that correspond to pressure P_1, e_2 is the void ratio of soil after compression and stabilization that correspond to pressure P_2, and a is the compressibility coefficient of soil.

4 Experimental results and analysis

4.1 Flaky stone experiment

The test results of flaky stone are presented in Table 5.

4.1.1 Basic working conditions

B1-1, B1-2, and B1-3 are three groups of parallel tests with 0.7-m thick flaky stone, and the compression curves are shown in Fig. 6.

Table 5 Comparison of experimental results of flaky stone under different working conditions

Working condition	Secant modulus (MPa)		110-kPa compression (mm)
	0–30/40-kPa external load	30/40–110-kPa external load	
B1-1	2.28	5.80	19.10
B1-2	3.33	6.44	16.20
B1-3	2.31	4.79	23.50
Average of B1-1, B1-2, and B1-3	2.64	5.68	
B1-4	3.84	8.20	12.60
B1-5	4.17	9.43	11.30
Average of B1-4 and B1-5	4.00	8.82	
B1-6	16.97	10.54	6.30
B1-7	13.53	9.83	7.10
Average of B1-6 and B1-7	15.25	10.19	
B1-8	10.82	6.44	11.20
B1-9	16.72	6.59	10.80

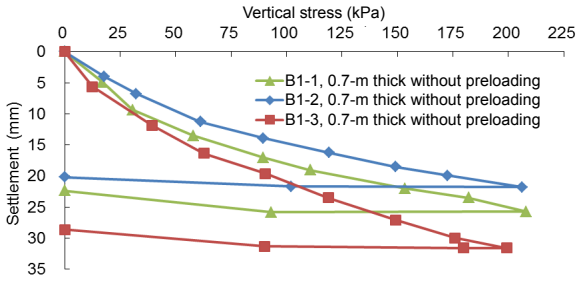

Fig. 6 Repetitive load–settlement curves of three parallel sets of 0.7-m thick flaky stone

The compression curve and the test results show that the test results are discrete due to the large particle size of the flaky stone, and the load displacement curve of the flaky stone exhibits a more apparent nonlinear change; however, the displacement increment gradually decreases with an increase in load, demonstrating more compression and higher density. When the external load is 0–40 kPa, the secant modulus is 2.28–3.33 MPa, with an average of 2.64 MPa. When the external load is 40–110 kPa, the secant modulus is 4.79–6.44 MPa, with an average of 5.68 MPa.

4.1.2 Influence of loading surface

The flaky stone is large. In the actual project, a 1-m thick gravel cushion can be laid on top of the flaky stone. Therefore, under B1-4 and B1-5 working conditions, the top of the flaky stone is leveled off with gravel, and the load–settlement curves are shown in Fig. 7.

The compression curve and experimental results show that the contact between the flaky stone and the loading plate is not as close as that between the gravel and the loading plate. The top surface is uneven, particle concentration is evident, and settlement is huge. When an actual force is applied, the flaky stone is passed through the gravel pad. The upper load is transmitted from the layer. Under B1-4 and B1-5 working conditions, the top surface of the flaky stone is leveled with 10-cm gravel, and the average secant modulus is 4.00 MPa for the load of 0–40 kPa, and 8.82 MPa for the load of 40–110 kPa.

4.1.3 Influence of preloading pressure

When laying the gravel cushion, the already laid flaky stone will bear the preloading effect of the gravel cushion chute and the self-weight load of the gravel cushion due to the effect of the height difference of the chute. On the basis of B1-4 and B1-5, two groups of parallel tests B1-6 and B1-7 are conducted. The applied preloading pressure of 40 kPa is used to simulate the drop pressure during the underwater laying of a 1-m thick gravel cushion. The load–settlement curves are shown in Fig. 8.

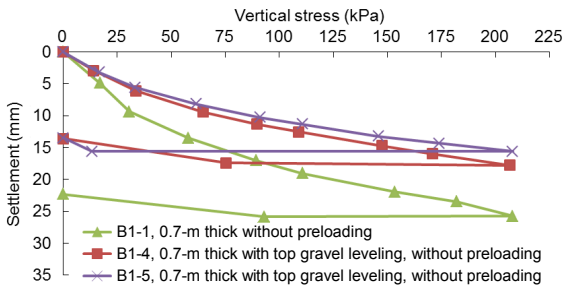

Fig. 7 Load–settlement curves of different loading faces

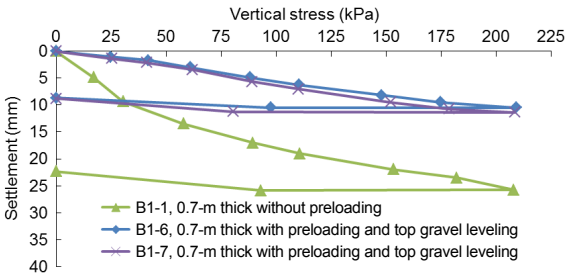

Fig. 8 Load–settlement curves under different preloading pressure conditions

The preloading pressure significantly affects the improvement of the initial stiffness of the flaky stone, reducing the initial settlement and overall settlement. After pre-pressing, the displacement from the 0 kPa to preloaded load segment is significantly reduced compared with the corresponding load segment without the preloading experiment. The secant modulus of the flaky stone is evidently increased due to the preloading. The secant modulus for load of 0–40 kPa is 13.53–16.97 MPa, with an average value of 15.25 MPa, which is 3.81 times the modulus in B1-4 and B1-5. The secant modulus for load of 40–110 kPa is 9.83–10.54 MPa, with an average value of 10.19 MPa, which is higher than the experimental results of B1-4 and B1-5.

4.1.4 Influence of flaky stone particle size

To study the influence of the particle size of the flaky stone on the compression performance of cushion, parallel experiments with two groups, i.e. B1-8 and B1-9, are conducted. The load–settlement curves are shown in Fig. 9.

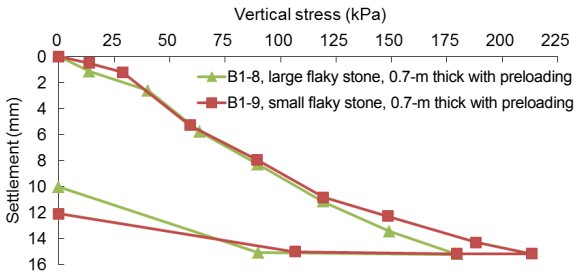

Fig. 9 Comparison of load–settlement curves of two different sizes of flaky stone

The size of the flaky stone is related to compression performance (the void ratio of the large flaky stone is 50.4%, and the void ratio of the small flaky stone is 48.5%). Under the same load, the settlement of the small flaky stone is slightly smaller than that of the large flaky stone, and their secant moduli exhibit minimal difference.

4.2 Gravel experiment

The test results for gravel are provided in Table 6.

B2-1, B2-2, and B2-3 are three groups of repeated parallel tests under the basic working conditions of the gravel cushion. The thickness of the B2-4 cushion is 1.7 m, and the other conditions are consistent with the basic working conditions. The compression curves are shown in Fig. 10. The experimental results are as follows.

1. The load–settlement curves of the three groups of parallel experiments have the same experimental results, which are relatively stable. Given the small gradation particle size of the gravel, the contact surface of the loaded plate is flatter and denser than that of the flaky stone. The breaking rate is not as high as that of the flaky stone, and the linearity of the compression curve is good. After pre-pressing via pipeline construction, the secant modulus is 23.64–27.82 MPa for load of 0–30 kPa, and 8.43–9.49 MPa for load of 30–110 kPa.

Table 6 Comparison of the gravel experimental results under different working conditions

Working condition	Secant modulus (MPa)		110-kPa compression (mm)
	0–30/40-kPa external load	30/40–110-kPa external load	
B2-1	23.64	8.87	9.55
B2-2	24.67	9.49	9.10
B2-3	27.82	8.43	10.30
Average of B2-1, B2-2, and B2-3	25.38	8.93	
B2-4	53.04	11.43	14.10

2. The preloading pressure generated by the gravel cushion considerably influences mechanical performance. The cushion is pre-compacted during the process (corresponding to the preloading curve) due to the preloading pressure of the material in the falling pipe. When the immersed tube is subjected to the pressure of the immersed tube bottom, the load–settlement curve is evidently gentler than the preloading curve before the force is applied to the previous preloading pressure, and the settlement under the same stress is significantly reduced. The average secant modulus is approximately 25.38 MPa. When the force exceeds the preloading pressure, the gravel is further compacted and the slope of the load–settlement curve increases. However, it still changes linearly, and the corresponding average secant modulus is approximately 8.93 MPa. The secant modulus of the four working conditions in the preloading stage is 4.31–4.73 MPa, with an average value of 4.49 MPa.

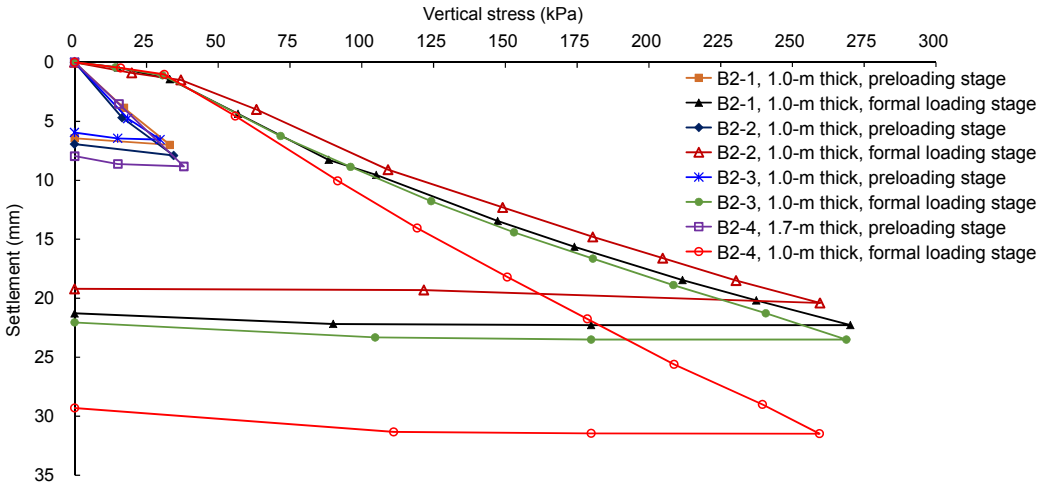

Fig. 10 Comparison of load–settlement curves under different working conditions

3. An increase in gravel thickness affects the modulus. The thickness of the gravel cushion increases from 1.0 m to 1.7 m or by 70%, and the compression modulus of the gravel cushion increases by 28%.

4.3 Flaky stone and gravel combination cushion experiment

The test results of the flaky stone and gravel combination cushion are presented in Table 7.

Table 7 Comparison of the experimental results under different working conditions

Working condition	Secant modulus (MPa)		110-kPa compression (mm)
	0–30-kPa external load	30–110-kPa external load	
B3-1	51.15	10.34	15.20
B3-2	46.63	10.60	14.50
Average of B3-1 and B3-2	48.89	10.47	
B3-3	69.93	11.99	14.10

B3-1 and B3-2 are two sets of parallel experiments under different working conditions. The gradation of the B3-3 flaky stone is 50–100 mm, and the other conditions remain the same. The compression curves are shown in Fig. 11. The results are as follows.

1. The change rule of the load–settlement curve of the two groups of repeated parallel tests of the flaky stone and gravel combination cushion is the same. The test result is relatively stable. The small gravel cushion can compensate for the gap of the flaky stone. The linearity of the curve is better than that for the flaky stone. The preloading pressure produced by laying the gravel cushion using the tube pass method has an evident effect on the mechanical performance of the composite cushion. By simulating the prepressure caused by the height difference in material construction, the secant modulus that is formally loaded at 0–30 kPa is 46.63–51.15 MPa, which is more than three times the secant modulus (10.34–10.60 MPa) loaded at 30–110 kPa.

2. The size of the flaky stone is related to its compression performance (the void ratio of the large flaky stone is 50.4%, and the void ratio of the small flaky stone is 48.5%). The settlement under the same stress of the two layers of small stone is slightly smaller than that of the large flaky stone combination cushion. The effect on the composite cushion modulus is small.

5 Conclusions

This study focused on the Shenzhen-Zhongshan Link immersed tube tunnel cushion and conducted experimental research on the major influencing factors of the flaky stone, gravel, and gravel and flaky stone combination cushion. The following conclusions can be drawn:

1. The size of the flaky stone is relatively large, indicating that the contact with the loading plate is not as close as that with gravel. When the top surface is

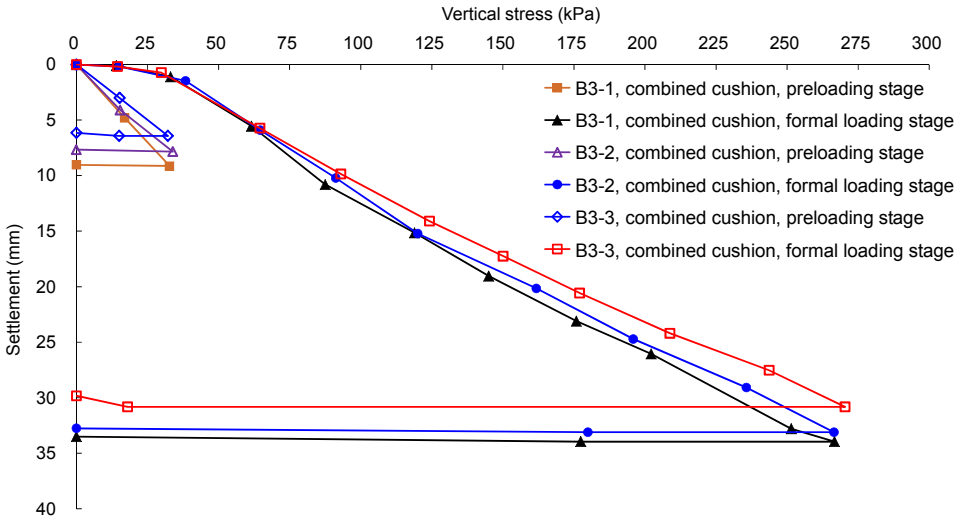

Fig. 11 Combined cushion parallel experiment load–settlement curves under basic working conditions

uneven, stress concentration on gravel particles is significant under the design load. The load–settlement curve exhibits nonlinear mechanical characteristics. The compactness of the cushion increases with external load. The gravel cushion particles are small. The top of the gravel cushion can be in close contact with the loading plate, and the bottom can fill the gap of the flaky stone. Thus, the load–settlement curves of the gravel cushion and the flaky stone and gravel combination cushion change linearly in two stages, and the stability of the composite cushion is better than that of the cushion containing only flaky stone.

2. The flatness and compactness of the top of flaky stone cushion considerably influence sedimentation and secant modulus. The comparison of the 10-cm gravel leveling experiment with the non-leveling experiment on the top surface of the flaky stone indicates that the settlement of the leveling flaky stone is reduced by 22.2%–51.9%, and the modulus is increased by 71.9%–86.9%. Thus, we recommend using a gravel cushion to fill the gap of the flaky stone before laying the gravel cushion on top of the flaky stone during construction.

3. The flaky stone gradation and the thickness of the gravel cushion influence the compression performance of the cushion, but the influence is not evident. The preloading of the pipeline construction exerts an apparent effect on improving the initial stiffness of the cushion, reducing the initial settlement and total settlement, and changing the load–settlement curve in two stages with preloading as the turning point. The average secant modulus with preloading pressure of 40 kPa is 15.25 MPa, which is 3.81 times the average modulus at the same stress level but without preloading.

4. Considering the preloading pressure of 30 kPa, the secant modulus of the combined cushion of 0.7-m flaky stone and 1.0-m gravel cushion is 48.89 MPa in the section of 0–30 kPa and 10.47 MPa in the section of 30–110 kPa.

Contributors

Wei-le CHEN is responsible for the overall planning of the project. Chao GUO and Jian LIU are responsible for the analysis and summary of the test data. Xiao HE and Bai-yong FU are responsible for the indoor model test and paper writing.

Conflict of interest

Wei-le CHEN, Chao GUO, Xiao HE, Bai-yong FU, and Jian LIU declare that they have no conflict of interest.

References

Chen JF, Zhou WX, 2013. Foundation treatment and application of submerged tunnel in Dalian Bay Project. Proceedings of Construction and Management of Underwater Tunnel, p.238-244 (in Chinese).

Feng HB, Yin G, 2018. Study of method of dredging construction for immersed tunnel with furrow gravel cushion foundation. *Tunnel Construction*, 38(1):86-90 (in Chinese). https://doi.org/10.3973/j.issn.2096-4498.2018.01.011

Fu QG, 2004. Development and prospect of immersed tunnels. *China Harbour Engineering*, (5):53-68 (in Chinese). https://doi.org/10.3969/j.issn.1003-3688.2004.05.017

Glerum A, 1995. Developments in immersed tunnelling in Holland. *Tunnelling and Underground Space Technology*, 10(4):455-462. https://doi.org/10.1016/0886-7798(95)00031-S

Grantz WC, 2001. Immersed tunnel settlements. Part 1: nature of settlements. *Tunnelling and Underground Space Technology*, 16(3):195-201. https://doi.org/10.1016/S0886-7798(01)00039-6

Gursoy A, 1995. Immersed steel tube tunnels: an American experience. *Tunnelling and Underground Space Technology*, 10(4):439-454. https://doi.org/10.1016/0886-7798(95)00032-T

He J, Xin WJ, 2019. Analysis and numerical simulation of abnormal siltation in foundation trench of immersed tube of Hong Kong-Zhuhai-Macao Bridge. *Advances in Water Science*, 30(6):823-833 (in Chinese). https://doi.org/10.14042/j.cnki.32.1309.2019.06.006

Li J, Li QF, Li B, 2002. Calculation and analysis of settlement of immersed tunnels controlling. *Journal of Zhengzhou University (Engineering Science)*, 23(3):94-97 (in Chinese). https://doi.org/10.3969/j.issn.1671-6833.2002.03.026

Li Y, Chen Y, 2011. The importance and technical difficulties of tunnel and islands for Hong Kong-Zhuhai-Macao Bridge project. *Engineering Mechanics*, 28(S2):67-77 (in Chinese).

Ranjith K, Narasimhan R, 1996. Asymptotic and finite element analyses of mode III dynamic crack growth at a ductile-brittle interface. *International Journal of Fracture*, 76(1):61-77. https://doi.org/10.1007/BF00034030

Rasmussen N, Grantz W, 1997. Chapter 9 catalogue of immersed tunnels. *Tunnelling and Underground Space Technology*, 12(2):163-316. https://doi.org/10.1016/S0886-7798(97)90021-3

Su ZX, Chen SZ, Chen Y, et al., 2018. Discussion on longitudinal static calculation of immersed tunnel. *Tunnel Construction*, 38(5):790-796 (in Chinese). https://doi.org/10.3973/j.issn.2096-4498.2018.05.011

Wang Y, 2015. An experimental study of deformation characteristics of gravel cushion for deeply immersed tube tunnel. *Rock and Soil Mechanics*, 36(12):3387-3392 (in Chinese). https://doi.org/10.16285/j.rsm.2015.12.007

Xie XY, Wang P, Li YS, et al., 2014. Long-term settlement monitoring data and finite element analysis of submerged tube tunnel in Yongjiang. *Rock and Soil Mechanics*, 35(8):2314-2324 (in Chinese). https://doi.org/10.16285/j.rsm.2014.08.026

Xu GC, Li YS, Sun J, et al., 1995. Foundation treatment of immersed tube tunnel, basement silting and foundation settlement. *Modern Tunnel Technology*, (3):2-18 (in Chinese). https://doi.org/10.13807/j.cnki.mtt.1995.03.001

Xu GP, Su QK, Li ZX, et al., 2015. Research on key design technology of extra-long immersed tunnel in open sea. *Highway*, 60(4):1-7 (in Chinese).

Xue JS, 2018. Study on the Consolidation Deformation Characteristics of Soft Soil and Settlement Calculation Method of the Soft Soil Foundation of Undersea Immersed Tube Tunnels under Repeated Desilting and Siltation Loading. MS Thesis, Beijing Jiaotong University, Beijing, China (in Chinese).

Yang GH, 2015. Foundation problems and challenges of the Hong Kong-Zhuhai-Macao Bridge tunnel. Proceedings of the 12th National Conference on Soil Mechanics and Geotechnical Engineering, p.213 (in Chinese).

Yang XL, Shao MH, Xu J, 2014. The overall scheme selection of rubble leveling for gravel cushion laying ship on Hong Kong-Zhuhai-Macao Bridge. *Construction Technology*, 43(11):17-19 (in Chinese). https://doi.org/10.7672/sgjs2014110017

Yue XB, 2014. Research on Settlement Characteristics and Calculation of Immersed Tube Tunnel with Soft Foundation and High Siltation. PhD Thesis, Chang'an University, Xi'an, China (in Chinese).

Zhang M, Wang XH, Yang GC, 2011. Numerical investigation of the convex effect on the behavior of crossing excavations. *Journal of Zhejiang University-SCIENCE A (Applied Physics & Engineering)*, 12(10):747-757. https://doi.org/10.1631/jzus.A1100028

Zhang XJ, Wei HB, Zhang JJ, 2013. Paving and leveling construction technology of immersed tube tunnel foundation from Pusan, South Korea. *Port & Waterway Engineering*, (6):177-182 (in Chinese). https://doi.org/10.3969/j.issn.1002-4972.2013.06.039

Zhang ZG, Fu BY, Liu XD, et al., 2018. General design and type selection of foundation bedding of undersea immersed tunnel for Hong Kong-Zhuhai-Macao Bridge. *China Harbour Engineering*, 38(1):34-38 (in Chinese). https://doi.org/10.7640/zggwjs201801007

Zhong HH, Li SG, Liu XS, et al., 2007. Comprehensive summary of research on sunk pipe tunnel. *Municipal Engineering Technology*, 25(6):490-494 (in Chinese). https://doi.org/10.3969/j.issn.1009-7767.2007.06.018

Zhou XR, Shen K, Li W, 2012. Preliminary study on model test of sand flow method for foundation treatment of Zhoutouzui Immersed Tunnel. *Technology Wind*, (14):128-129 (in Chinese). https://doi.org/10.3969/j.issn.1671-7341.2012.14.106

中文概要

题　目：沉管隧道碎石垫层力学行为与变形特性试验研究

目　的：目前国内外尚无采用二片石+碎石作为沉管隧道先铺法垫层的先例，且二片石+碎石组合垫层的力学变形特性尚不明确。本文旨在通过室内物理力学模型试验，定量分析二片石及碎石垫层铺设厚度、级配、落管预压荷载量等因素的影响，提

出碎石垫层构造方案以及相应的变形模量和承载力等力学指标，以合理确定垫层厚度及可行的施工工艺、准确评估地基刚度偏差、降低淤泥对碎石垫层承载性能的影响以及保证沉管结构的受力安全。

创新点： 1. 提出二片石+碎石组合垫层的力学变形特性；2. 提出落管预压荷载的作用以及对垫层性质的影响。

方　法： 1. 分别开展二片石和碎石的室内物理力学模型试验，研究二片石与碎石接触面的平整度、颗粒级配、落管预压荷载以及垫层厚度对垫层的物理力学性质的影响，并在此基础上开展二片石+碎石组合垫层的室内模型试验；2. 提出碎石垫层构造方案以及相应的变形模量和承载力等力学指标，以提高沉管结构的受力安全。

结　论： 1. 在设计荷载作用下，二片石垫层的荷载-位移曲线呈现越压越密的非线性受力特点，而碎石垫层和碎石+二片石垫层的荷载-位移曲线呈现两阶段线性变化；2. 二片石垫层顶部的平整密实度对其沉降和压缩模量有很大的影响，因此在施工时需保证二片石垫层顶部的平整密实度；3. 级配和厚度对垫层的压缩性影响不明显，而落管预压荷载对提高垫层初始刚度以及降低初期沉降和总体沉降有明显作用；4. 对于预压荷载为 30 kPa 的 0.7 m 二片石+1.0 m 碎石组合垫层，压缩模量的取值在 0~30 kPa 段为 48.89 MPa，在 30~110 kPa 段为 10.47 MPa。

关键词： 沉管隧道；碎石垫层；模型试验；变形特性